Aspects Regarding the Performance of Differential Current Measurement

Cornel Stanca [1], Lia Elena Aciu [2]

[1]*Transilvania University of Brasov,, Electronic and Computers Department, Bdul Eroilor 29, Brasov, Romania*
[2]*Transilvania University of Brasov,Electrical Engineering and Applied Physics Department, Bdul Eroilor 29, Brasov, Romania*

Abstract **– In this paper is presented the study on Hall current sensors for differential current measurement, aiming to be used in a smart protection device for leakage current in low voltage lines. Experiments have highlighted solutions but also various deficiencies. The paper also proposes measures to enhance measurement errors.**

Keywords **– Smart protection devices, differential current, Hall current sensor.**

1. Introduction

The introduction of microprocessor-based protective system brings facilities and features which have no parallel in conventional technologies. In particular, digital relays can be programmed to provide post-fault analysis and observed all the transient phenomena. This is achieved by reading out sampled data that have otherwise been acquired as part of the fault-measurement process [1]. The flexibility of a microcontroller-based protection system allows, after an event to reconnect the power supply automatically, in certain established conditions [2].

DOI: 10.18421/TEM64-21
https://dx.doi.org/10.18421/TEM64-21

Corresponding author: Lia Elena Aciu,
Transilvania University of Brasov,Electrical Engineering and Applied Physics Department, Brasov, Romania
Email: lia_aciu@unitbv.ro

Received: 22 September 2017
Accepted: 02 November 2017
Published: 27 November 2017

Differential protection calculates the sum of all current flowing into and out of the protected object. Apart of magnetizing currents and capacity charging current, this current sum must always be equal to zero if the protected object is un-faulted. Internal faults are therefore detected by the appearance of a differential current [3].

In power protection systems, differential relay operates when there is a difference between two or more similar electrical quantities and exceeds a predetermined value. The most common is the differential current protection relay. They are very sensitive to the fault occurring within the zone of protection but they are least sensitive to the faults that occur outside the protected zone [4].

A theoretical evaluation of a novel, all-optical differential current protection scheme employing low voltage piezoelectric transducers, fiber Bragg grating sensors and Rogowski coils is presented in [5].

A differential current-based fast fault detection and accurate fault distance calculation is proposed for photovoltaic (PV)-based DC micro-grid by [6].

Reference [7] proposes a novel transverse differential protection for voltage sourced converter-high-voltage, direct current (VSC-HVDC) to clear faults on DC-line fast. The proposed scheme depends on the transient current of positive pole and negative pole at the same side. Transverse differential current can be used to distinguish DC and AC faults, novel criteria are built using the ratio of difference and sum the current of bipolar. According to the variation characteristics of transient fault current, the internal faults and external faults can be detected. The scheme can protect the whole transmission line without dead zone, simplify the algorithm and improve the speed of operation.

A circuit breaker is both a circuit-breaking device that can make, withstand and break currents whose intensity is at most equal to its rated current (I_n), and a protection device that can automatically break over-currents which generally occur following faults in installations [8].

Protection against electric shock at mains voltage and from indirect contact consequent to the earth fault may be provided by means of the excess current

protection. It will be satisfactory if the earth loop impedance is sufficiently low for enough fault current to flow to operate the protective device within the recommended time [9].

The smart protection devices is an important class of devices used today in smart grid city home devices and it eliminates over-voltages in differential mode, between phase and neutral. In these devices there are current sensors with different operating principles, different design variants, different performances and cost prices. A smart device that encompasses almost all the protective functions of undesired events in a low-voltage power supply network includes, among other things, over current protection (high currents), short circuit (very high currents) and differential current (low current). Sensors designed to measure leakage current are an integral part of the differential circuit breaker.

Differential circuit breakers are found under various names such as Residual Current Circuit Breakers in Canada and GFCI (Ground Fault Circuit Interrupter) or ALCI (Applied Leakage Current Interrupter) in the US and are regulated by the standard IEC 60755 (General requirements for residual current protective device). From the point of view of sensitivity (current sensors), the differential circuit breaker according to the standard can be classified into: high sensitivity - 6,10,30mA - for human protection (HS class), with medium sensitivity - 100, 300, 500, 1000mA - for fire protection (MS class) and low sensitivity - 3, 10, 30A - for protection of equipment (class LS) [10].

There are two variants to determine the differential current that can occur in low voltage power supply lines:

1. The use of two current sensors appropriate to the load current range (currents in the order of tens of amps), one for the phase current and the other for the current on the neutral and their connection to the input of a differential amplifier. Although the solution seems to be advantageous in terms of the performance of the sensors used in the load current working range (as well as the very low gauge for integrated circuit sensors), its own noise makes it impossible to highlight small currents (as is the case with leakage to the ground). For example, for the integrated sensor ACS712 (Allegro) with effect Hall, for input current ranges of ± 5...± 30A, the sensitivity is 66...185 mV /A and its own noise of 7... 21 mV. This result in the minimum value of the current that can be emphasized and is about 110mA, well above the value of the drain currents that can trigger the protection circuit (30mA standard). Noise simply drowns the useful signal if no additional shielding measures are taken. Additional protection and the use of high-precision components can make it possible to measure, however, with high costs.

2. The use of a Hall sensor with hole through which both conductors (phase and neutral) pass. In this way, only the difference in magnetic flux generated by the currents on the load circuit will generate the sensor output current. By selecting the appropriate resistance of the reaction, the sensitivity of the sensor changes so that currents in the order of tens of mA can be detected with good accuracy. There are good-performing implementations such as DRY421 (Texas Instruments) or CYCS11-nx drain current transducers. Since the gauge of these leakage current transducers is too large for smart applications requiring multiple protections in a small space, the use of a current sensor used for the load current has also been analyzed.

Nowadays, there are used zero-phase current transformers (ZCT) [11] that solve the difficulties of accurately measuring small differential currents. The disadvantage of this solution is the high price.

Lately, the moulded-case circuit breaker (MCCBs) for LV applications is designed to protect applications in commercial and industrial buildings [12]. These circuit breakers are suitable for isolation, guaranteed to IEC 60947-2, and provide a highly visible and lockable contact position indicator to ensure operator confidence. Extended current limiting and thermal protection can reduce the stresses on equipment due to short circuits and their associated effects. Earth leakage protection can be added by installing a Vigi CVS option module. In the event of a circuit fault, simple visual indicators help to locate the tripped breaker and take steps to correct the problem.

2. Study of behavior of Hall current sensors used to measure differential current

2.1. Equipment, devices and method

The current sensor with Hall effect was used, both for load current and differential current, TELCON HTP25 (UK) with the following features: Rated Primary Current - 25A, Turns Ratio - 1000:1, Rated Power Supply ±15V ±5%, Linearity 0.1% of rated primary current, Overall Accuracy 0.5% of rated primary current, Output Zero Adjustment <±200μA at primary current=0A, Zero Offset/Temperature<5μA/°C, Zero Offset/Supply Variation<5μA/V, Bandwidth (-1dB)dc to 200kHz min., di/dt following>200A/μs, Delay Time0.1μS, dV/dt Immunity10kV/μs. The sensor has a central hole for passing of the conductor / conductors crossed by the measured current - the primary coil. Measurement of load current and differential current was achieved with the TEKTRONIX TDS 3034B eScope oscilloscope with the following characteristics: Analog Bandwidth - 300MHz, Sample rate - 2.5GS / s.

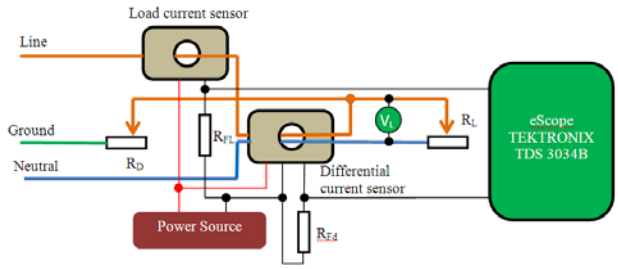

Figure 1. Measurement circuit

The experimental assembly is shown in Figure 1., where R_{FL} - feedback resistor for load current sensor, R_{Fd} - feedback resistor for differential current sensor, R_L - load resistor (variable in steps), R_D - resistor used for emulating the leakage current (variable in steps).

For measuring the differential current, the same type of sensor was used as in the case of load current measurement but with passing both conductors (phase and neutral) through the central hole in the same direction.

The voltage monitoring on the load was done with the voltmeter V_L. During the experiments, the voltage had the measured value of 237V ± 0.25%.

2.2. Experiments' goals and results

The experiments aimed at:

1. Determining the dependence between the differential current measured with the sensor and the load current;
2. Finding the optimal design for the differential current sensor.

Experiments were conducted for the following specifications:

- 3 configurations relative to the number of primary coil: 1, 2 and 3 turns. The number over 3 could not be increased due to the limited size of the central hole;
- 6 differential current I_d values: 5, 10, 15, 20, 25 and 30mA;
- load current values: 0…12A.

Experiments were done to determine the dependence between the normalized measured differential current and the load current (Id set at 5, 10, 15, 20, 25, 30mA) when using a primary coil with one turn (Fig.2.), two turns (Fig.3.) and three turns (Fig.4.).

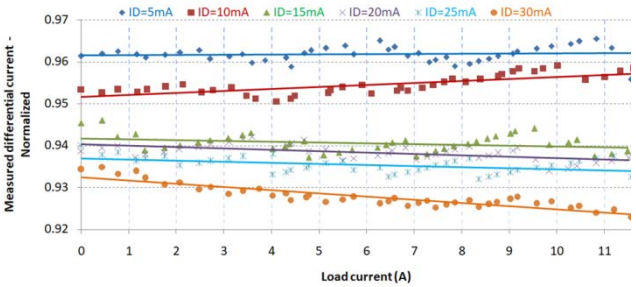

Figure 2. Normalized measured differential current depending on the load current for I_d=5, 10, 15, 20, 25 and 30mA using a primary coil with one turn

From Figure 2., it can be observed that there is a monotone decrease of the differential current measured for no loads with the increasing set value of the differential current. Also, maintaining relatively low values of the slope of the linear characteristic with which each of the measured values is set. The non-linearity errors are very high 22 - 58% and the correlation coefficients very low, 0.08 - 0.84.

In the case of two turns (Fig.3.) the nonlinearity errors are still large 6 - 40% but the correlation coefficients are much higher than in the case of a single spiral in the primary, 0.6 - 0.98.

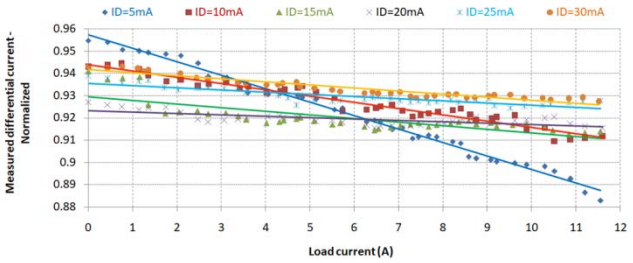

Figure 3. Normalized measured differential current depending on the load current for I_d=5, 10, 15, 20, 25 and 30mA using a primary coil with two turns

For three turns (Fig.4.), the nonlinearity errors are lower, 9 - 20%, and the correlation coefficients are high, 0.92 - 0.98.

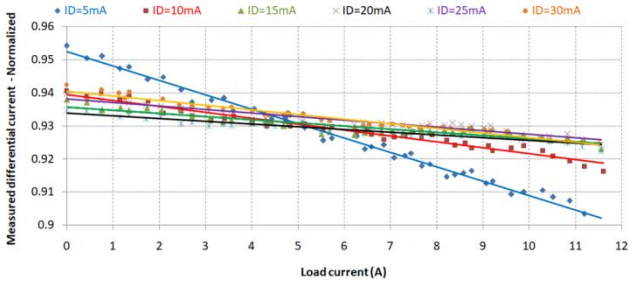

Figure 4. Normalized measured differential current depending on the load current for I_d=5, 10, 15, 20, 25 and 30mA using a primary coil with three turns

The decrease of the differential current measured for no load, with the increase of the set differential current is no longer monotone. The slope of the linear characteristic can be approximated as high - at low differential currents and greatly decreases for the increase of the differential current. The nonlinearity and dispersion error values become reasonable.

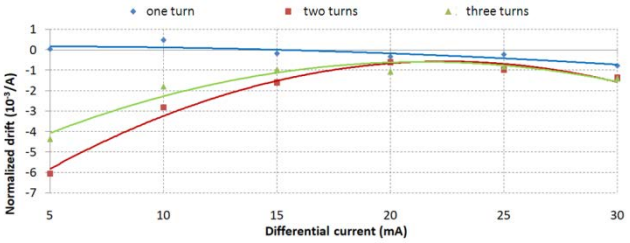

Figure 5. Normalized drift of differential current depending on set value of differential current, for three values of primary coil turns

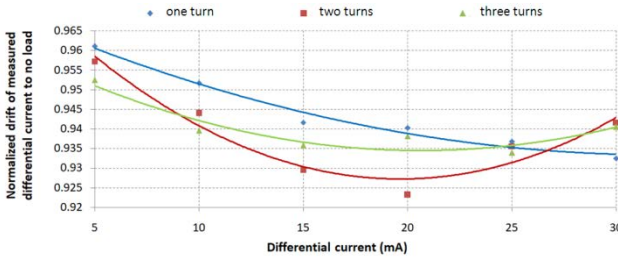

Figure 6. Normalized drift of measured differential current to no load depending on set value of differential current for three values of primary coil turns

The comparative analysis of the behavior of the differential sensor having one, two or three turns is synthesized in Figure 5. and Figure 6.

For all three situations, the dependence is square, of the form (1):

$$y = a_2 \cdot x^2 + b_2 \cdot x + c_2 \qquad (1)$$

Figure 6. shows the dependence of the deviation of the differential current measured by the sensor in the absence of load (on y axis) by the differential current (x axis).

It can be observed a quadratic, a same form given the equation (1), and the values of the coefficients are given in Table 1.

The correlation coefficient (R^2) quantifies how the equation (1) approximates the set of measured values.

Figure 7. shows the dependence of the slope deviation of the linear characteristics that approximate the I_{dmN} (I_L) dependencies of the current sensors. On y axis is the slope of the normalized measured differential current, on x axis is the set differential current and a_2, b_2 and c_2 are coefficients whose values are given in Table 1.

Table 1. Comparative analysis of sensors with different number of primary coil turns and different values of differential current

Figure number	Number of turns	Coefficients			
		a_2	b_2	c_2	R^2
7	1	-0.000893	-0.009036	0.355	0.7708
	2	-0.01745	0.55329	-9.295	0.9815
	3	-0.01294	0.78104	-6.51	0.9357
8	1	0.00004	-0.00237	0.97151	0.9777
	2	0.00015	-0.00574	0.9836	0.9334
	3	0.00007	-0.00281	0.96345	0.8773

The analysis of the values from Table 1. and the curves of Figure 5. and Figure 6. reveal that the best correlation coefficient is obtained for the primary two turns sensor, although this variation exhibits the highest values of the deviations for most of the set differential currents.

The high correlation coefficient makes the differential current sensor with two primary turns the most appropriate if the measured values are compensated in the processors using a deterministic algorithm and the differential current measured is in the range of 5-30mA.

Figure 5. shows that by using two or three turns in the primary winding, a minimum slope is obtained between if the differential current I_d is set between 20 and 25mA while in Figure 6. it results that at 20mA value, for both configurations, the deviation at zero load current of the measured value is maximal.

Since in the protection circuits the value I_d = 30mA is the threshold value at which the circuit triggers, Figure 7. compares the behavior of the differential current sensor set to this value for one, two and three primary turns.

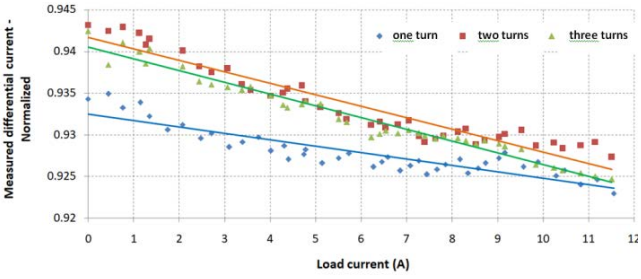

Figure 7. Normalized measured differential current depending on load current for 30mA actual value of differential current and for three values of primary winding's turns

Table 2. lists the values of linear equation coefficients

$$I_{dmN} = a_1 \cdot I_L + b_1, \quad (2)$$

which approximates the characteristics of I_{dmN} (I_L) and the value of the correlation coefficient R^2.

$I_{dmN} = \frac{I_{dm}}{Id}$ is the normalized measured differential current (I_{dm} being the differential current measured in mA),

I_L(A) - the load current,

a_1 – the slope of the normalized linear characteristic,

b_1 – the value of the differential current normalized to the zero current in the load.

Table 2. Comparative analysis of sensors with different number of primary winding's turns for 30mA differential current

Number of turns	Coefficients		
	a_1, (mA·mA^{-1}·A^{-1})	b_1, (mA·mA^{-1})	R^2
1	-0.00076	0.9324	0.803
2	-0.00138	0.9416	0.912
3	-0.00141	0.9405	0.964

In conclusion, in the case of calculating the measurement error compensation by deterministic algorithms, the most suitable is the sensor with three turns in the primary coil, even if it does not offer the best values of slope and value deviations, to zero current in the load.

3. Solutions to improve the performance of differential current determination using Hall sensors

3.1. Hardware solutions

For the triggering value of I_d=30mA, a hardware solution that compensates the errors can be used as in Figure 8. U1:A is used as a non-inverting summing operational amplifier. The zero load current deviation (coefficient b_1 in Table 2.) is determined by the potentiometer R_0 and the resistors R_2 and R_3 and the deviation at the rated currents (coefficient a_1 in Table 2.) by the resistors R_1 and R_2.

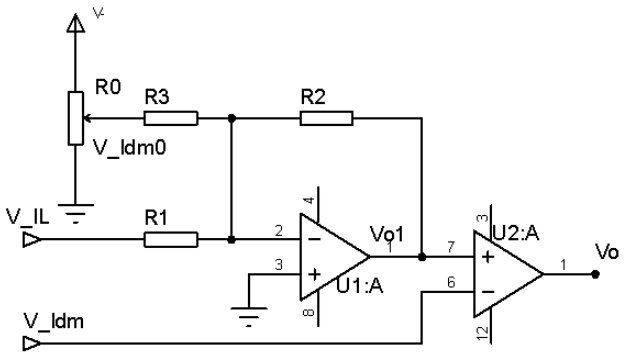

Figure 8. Triggering circuit at threshold overcome of differential current

In this case, the linear characteristic of the new circuit has the expression (3):

$$V_{o1} = -(\frac{R_2}{R_1} V\_IL + \frac{R_2}{R_3} V\_Idm0), \quad (3)$$

where: *V_IL* is the voltage at the output of the load current sensor I_L. For R_{FL}=500Ω and input range 0-10A will correspond to the output range 0-5V;

V_Idm0 is the voltage measured from the output of differential current sensor for zero load current, I_{dm0} (constant value, experimentally determined). For R_{Fd}=*100k*Ω and the input range 0-30mA will correspond an 0-3V output range. It can be noted that the voltage *V_ID0* is negative, so that the free term in equation (3) will be positive.

From (2) and (3) it follows that

$$\frac{R_2}{R_1} = \frac{a_1 \cdot I_d \cdot R_{Fd}}{R_{FL}} \quad \text{and} \quad \frac{R_2}{R_3} = b_1.$$

Thus, for the coefficients determined in Table 2. and the resistance value of R_2=1kΩ, the result is R_1=118kΩ şi R_3=1.06kΩ.

U2:A is a threshold comparator circuit. On the non-inverting input voltage V_{o1} is applied from the output of the circuit U2:A of the form (3), and at the inverting input the voltage *V_Idm* from the output of the differential current sensor with R_{Fd}=*100k*Ω..

The operation of the circuit in Figure 8. is described by the characteristic from the Figure 9.

At voltage values *V_Idm* from the differential current sensor output in the hatched field, the output of the circuit is 1 logic, meaning that there is no leakage current greater than 30mA so the power supply is not cut off.

If the *V_Idm* voltage value is outside the hatched area, the leakage current is over 30mA, then *Vo*=0 and the protection circuit triggers (stops the power supply).

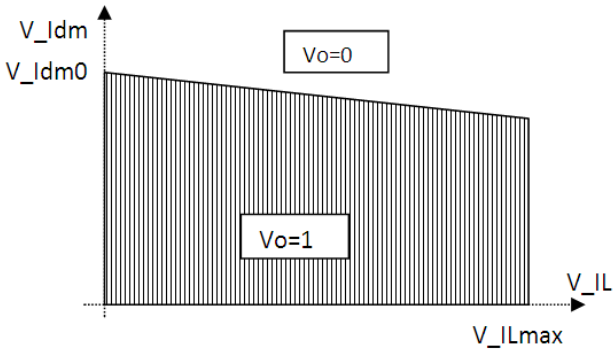

Figure 9. The circuit's (from Figure 8)characteristic

3.2. Software solutions

For the microcontroller based protection systems the determination of the differential current (which will cause the associated fault event to be declared or not) can be made by:

1. Using a LUT (Lookup Table) with the experimentally determined I_{L_LUT} şi I_{d_LUT} (Table 3.) values of load current and differential current. The steps are:

- It is calculating the value of the differential current I_{d_c} (which depends on the load current value) corresponding to the measured I_L, load current using the linear interpolation (4):

$$I_{d\_c} = I_{d\_LUT}(i-1) + \frac{I_{d\_LUT}(i) - I_{d\_LUT}(i-1)}{I_{L\_LUT}(i) - I_{L\_LUT}(i-1)} \cdot [I_L - I_{L\_LUT}(i-1)] \quad (4)$$

- The value is compared to the measured value of the differential current I_{dm}. If $I_{dm} \geq I_{d\_c}$ .there is an excess from the limited value, an event is declared and the power supply is switched off.

Table 3. LUT for values of load current and differential current

Index	$I_{L\ LUT}$	$I_{d\ LUT}$
i=1	*0*	I_{dm0}
…	…	…
i=n	I_{Lmax}	$I_{dm\ ILmax}$

2. By calculating the differential current I_{d_c} corresponding to the measured current load I_L.

Used is the linear experimentally determined equation (5):

$$I_{d\_c} = a_1 \cdot I_d \cdot I_L + b_1 \cdot I_d, \quad (5)$$

where a_1 and b_1 are the coefficients in Table 2, I_d=30mA. The obtained value is compared with the measured value of the I_{dm} differential current. As in the previous case, if $I_{dm} \geq I_{d\_c}$, an event is declared and the power supply is switched off.

Sources of experimental measurement errors were also determined. The most important of these are:

- The position of the conductors (phase and null) near the sensor, Figure 10.

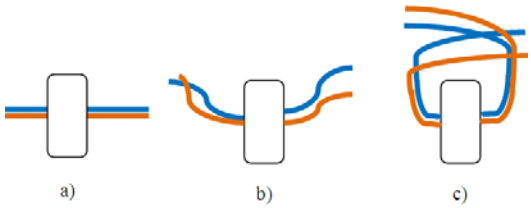

Figure 10. Three different positions of primary turns: a) normal position, b) and c) positions which generate errors

- The unequal size of the phase and neutral section's turns (the largest errors), Figure 10. Minimizing this type of error was done by using of twisted yarn pairs as primary winding conductor, Figure 11.

Figure 11. Differential current sensor with twisted yarn pair for primary winding

4. Conclusion

It has been determined that Hall sensors with two or three turns in the primary coil have a better precision and behavior and that can be very well approximated by mathematical functions, so they are indicated in deterministic algorithms.

The best approximation of mathematical functions was made for the sensor with three turns in the primary coil designed to measure the 30mA differential current.

Due to the limited size of the sensor's center hole, the number of turns of the primary coil could not be increased more than three.

By increasing the Hall sensor's reaction resistance to the upper limit, it increases its sensitivity with positive effects on accuracy.

Hardware and software solutions for error correction have been proposed.

In the case of software solutions, it is proposed to use a LUT (I_L, I_d) generation or to determine the $I_d(I_L)$ characteristic. In this case, continuous or stepwise loading over the entire range ($0…I_{Lmax}$) will be injected, and the value for the pairs (I_L, I_d) will be read.

Acknowledgements

The paper is based on the research done within the frame of the project 62PED/2017.

References

[1]. Johns Salman, A.T. & Salman. K. (1995). *Digital protection for power systems.* Peter Peregrinus Ltd.

[2]. Romanca, M. & Ogrutan, P. (2011). *Embedded computer systems. Applications with microcontrollers.* Transilvania University Press.

[3]. Ziegler, G. (2012). *Numerical differential protection: principles and applications*. John Wiley & Sons.

[4]. Muddebihalkar, S. V., & Jadhav, G. N. (2015, December). Analysis of transmission line current differential protection scheme based on synchronized phasor measurement. In *Power, Control, Communication and Computational Technologies for Sustainable Growth (PCCCTSG), 2015 Conference on* (pp. 21-25). IEEE.

[5]. Nasir, M., Dysko, A., Niewczas, P., Booth, C., Orr, P., & Fusiek, G. (2013, September). Development of power system differential protection based on optical current measurement. In *Power Engineering Conference (UPEC), 2013 48th International Universities'* (pp. 1-4). IEEE.

[6]. Snehamoy Dhar; S. & Dash, P.K. (2017). Differential current-based fault protection with adaptive threshold for multiple PV-based DC microgrid, *IET Renewable Power Generation, 11*(6), 778-790.

[7]. Shilong Li, S., Chen, W., Yin, X., & Chen D. (2017). Protection scheme for VSC-HVDC transmission lines based on transverse differential current, *IET Generation, Transmission & Distribution, 11*(11), 2805- 2813.

[8]. Siemens, Ltd. (2009).*Breaking and protection devices - Power Guide*. Legrand.

[9]. Oldham Smith, K. & Madden, J.M. (2002). *Electrical Safety and the Law: A Guide to Compliance*, Blackwell Science Ltd.

[10]. Ogrutan, P., Aciu, L., Lozneanu, D., Rosca, I.& Munteanu, *R. (2011). Electronic Interrupter and leakage current protection method*. OSIM Patent request no. A00880.

[11]. Yuecheung Chung, G. (2007). *Electric shock prevention residual circuit breaker*. US patent no.0215576 A1.

[12]. Schneider Electric (2017). Moulded-case circuit breakers for buildings, *Technology & business for development*,
Retrived from:
http://www.ee.co.za/article/moulded-case-circuit-breakers-buildings.html , (accessed 05 June 2017).